C302: MODELLING OF FLEXIBLE PAVEMENTS WITH THIN BITUMINOUS SURFACING – Using Linear elastic theory and FINITE ELEMENT Method

G. CHAI[5], H. GUAN, **R. C. VAN STADEN**[6], K. WHITTAKER and Y. C. LOO

Griffith School of Engineering, Griffith University, Queensland, Australia

ABSTRACT

Flexible road pavements are important transport infrastructure in Australia for providing an all weather road network for a population of 22 million people with land size of about 7 million square kilometres. Between the surfacing types, sprayed seal and thin asphalt are most commonly used by State and Local Governments for rural road construction. Asphalt fatigue and subgrade deformation from repeated loading over time are the most common failure mechanisms and these in turn are the major attributors to the pavement maintenance and rehabilitation cost. Thin surfacing pavements with a weak road base and foundation often exhibit plastic deformation in the base and subgrade layers. Linear Elastic Theory (LET) and Finite Element Method (FEM) based numerical analyses have been widely used in research to develop pavement models and replicate realistic vehicular loadings. The thin surfacing pavement is modelled using LET and FEM with three-dimensional (3D) ideal elastic layered system and two-dimensional (2D) axisymmetrical elements, respectively. The vertical displacements at the top of the asphalt layer are determined using both LET and FEM and the findings compared to the measured field data. Results show that the deflections generated by the FEM are in closer agreement with the field data. At a horizontal distance of 700 to 1500mm from the loading significant displacement variances from the field data are found for both LET and FEM.

KEY WORDS
flexible pavement, linear elastic theory, finite element method, displacement characteristics.

INTRODUCTION

Construction and maintenance of an adequate and efficient road network is amongst the most important infrastructural priorities of a country. A pavement is designed to provide safe and long-lasting road surfaces. However, fatigue and deformation from

[5] Corresponding author: Email: g.chai@griffith.edu.au
[6] Presenter: Email: r.vanstaden@griffith.edu.au

repeated vehicular loading over time are the most common failure mechanisms and the major attributors to pavement maintenance and rehabilitation costs. Thus, pavement performance predictions are fundamental for improving design and construction of pavement systems. Figure 1 illustrates a three layer flexible pavement system with an asphalt layer as the top surface and the subsequent base course, subgrade and natural foundation. Also shown in the figure is the vehicular loading and tyre contact surface.

Burmister (1943) was the first to apply Linear Elastic Theory (LET) of continuum mechanics in both two and three-layer pavement systems for determining stresses, strains and displacements. This method is termed mechanistic because it uses the concepts of mechanics to derive stress, strain or deflection. One of the computer programs based on Burmister's theory is ELSYM5 (Kopperman et al. 1986) featuring a three-dimensional (3D) ideal elastic layered pavement system. Heath et al. (2003) stated that programmes based on LET are more accurate, efficient and easy to use when compared to Finite Element Analysis (FEA) software because there is no need to generate complicated three-dimensional meshes and there are relatively lower requirements for computational time and memory. However, FEA software has been effectively used to evaluate pavement behaviour more accurately under a wide range of different material properties and traffic load conditions (Dondi 1994). To date, no published research appears to have compared pavement deflection measurements from field data with those from both LET and FEA.

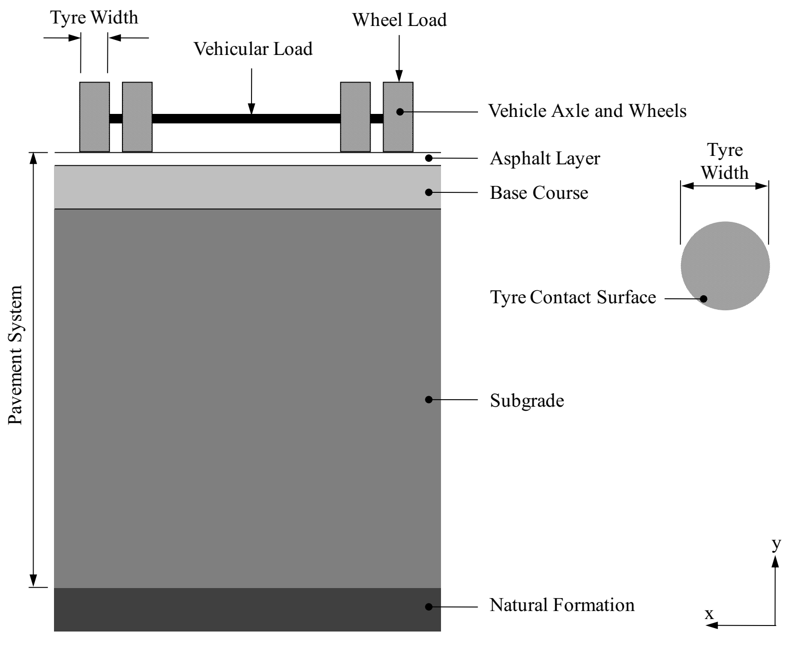

Figure 1: Flexible pavement system and vehicle loading.

METHODOLOGY

The modelling and simulation herein are performed using ELSYM5 (Kopperman et al. 1986) (model one, M_1) and Strand7 Finite Element Analysis (FEA) System (2004) (model two, M_2). The performance of M_1 and M_2 is compared against ten field data sets collected at various locations of the wheel path. Each field data set exhibits different layer thicknesses, t and Young's moduli, E. The field data is obtained from a section of flexible granular pavement in South East Queensland, Australia that has low traffic loading with an average daily vehicle usage of 250. A falling weight of 20kN is positioned over a 300mm diameter section of the pavement and a falling weight deflectometer (FWD), mounted on a trailer, is used to measure the vertical displacements at the top surface of the asphalt layer.

The t of all layers and E of the subgrade are determined through coring at the same ten locations used when measuring the displacements. However, E of the asphalt and base course must be determined before the performance of M_1 and M_2 can be compared against the field data. A well established technique for determining E of the field data is through back calculation (Lytton, 1989). Back calculation is an iterative procedure of matching actual measured vertical displacements, obtained from field data, with calculated values through the use of LET and FEM. Since both M_1 and M_2 have linear material properties the calculated displacement characteristics will not precisely match the nonlinear behaviour of the field data.

The first iteration of the back calculation procedure involves estimating a E value only for the asphalt layer (i.e. E_A) and calculating the displacements using LET and FEM. The actual displacements are then compared with the calculated and a correction made to the initial estimation of E_A. This procedure is repeated until the error differences between the actual and calculated values are small enough to be neglected. The second cycle of iterations are then performed by varying E of the base course (i.e. E_B). It is noticed that significant alterations in E_A and E_B, results in minor changes in the displacement characteristics and therefore, in an attempt to keep E_A and E_B in a plausible range, E of the subgrade (i.e. E_S) is varied. The order in which the layers are evaluated does not necessarily influence the final prediction of the displacement magnitude and distribution. In accordance with Austroads (2004) the ranges of E_A, E_B and E_S used during the back calculation procedure are 15-120MPa, 80-600MPa and 2000-4000MPa, respectively. Increments for varying E_A, E_B and E_S are respectively 1, 5 and 100MPa. The E of each layer that provides vertical displacement characteristics closest to the field data sets are provided in Table 1. Note that the subgrade thickness (i.e. t_S) is constant at 5000mm for M_1, M_2 and field data.

Modelling

Illustrated in Figure 2 are the two models considered in this study, including vehicular loading details. M_1 is represented through a three-dimensional (3D) elastic multilayered model and M_2 a two-dimensional (2D) axisymmetrical finite element model. Three types of layers, i.e. asphalt layer, base course and subgrade, are defined and full friction is assumed at the boundaries for both M_1 and M_2.

For M_1 each layer is assumed to be composed of a weightless, homogeneous, isotropic material (Uddin et al. 1994). Each layer is of uniform thickness and infinite width in all horizontal directions. The bottom elastic layer is semi-infinite in thickness. The boundaries between the layers are assumed to have full friction and the surface free of shear. Vehicular loading is assumed to be uniformly distributed over a defined circular surface area. These modelling assumptions of M_1 will contribute to differences in the back calculated t and E of all layers, when compared to that of M_2.

M_2 differs from M_1 by possessing restraints applied to both the outside edge and the bottom edge of the pavement system. The outside edge is restrained from rotating around the x- and y-axes and translating through the x- and z-axes (i.e. roller). The bottom edge of the pavement is restrained from deforming in any direction. Note that the x-axis is the radial axis and the nodes that lie on the symmetry axis (y-axis) (see Figure 2 b)) have only one degree of freedom, translation in the y direction. The finite element model, M_2 also differs from M_1 by making use of stiffness matrixes with boundary conditions and by requiring mesh definition. For M_2 that best satisfies field data set 5, as an example, the total number of triangular and quadrilateral axisymmetrical elements are 200 for the asphalt layer, 550 for the base course and 2550 for the subgrade. The total number of nodal points for the entire pavement model is 3329. As indicated in Figure 2, the vertical displacement is measured along the line TT for both M_1 and M_2. The beginning location of line TT is identified as TT_1 and the end as TT_2. TT_1 begins at the centre of the applied loading and extends horizontally for 1500mm. These locations are prone to plastic deformation under traffic conditions.

A single wheel load of 20kN representing an equivalent 80kN standard axle load is assumed. The effect of the air pressure within the tyre is neglected, hence the contact pressure of the tyre is assumed to be uniformly distributed. The force of 20kN is represented as a single static pressure of 282.55kPa applied to a circular area with a diameter of 300mm for M_1 and as an edge pressure acting on the plate element, and extending 150mm from the symmetrical axis, for M_2 (see Figure 2). The material properties (i.e. E and t) specific to field data, M_1 and M_2 are given in Table 1. The Poisson's ratios, v are assumed to be 0.4, 0.35 and 0.45 respectively for the asphalt layer, base course and subgrade of both M_1 and M_2. All material properties are assumed to be linear, homogeneous and elastic in behaviour.

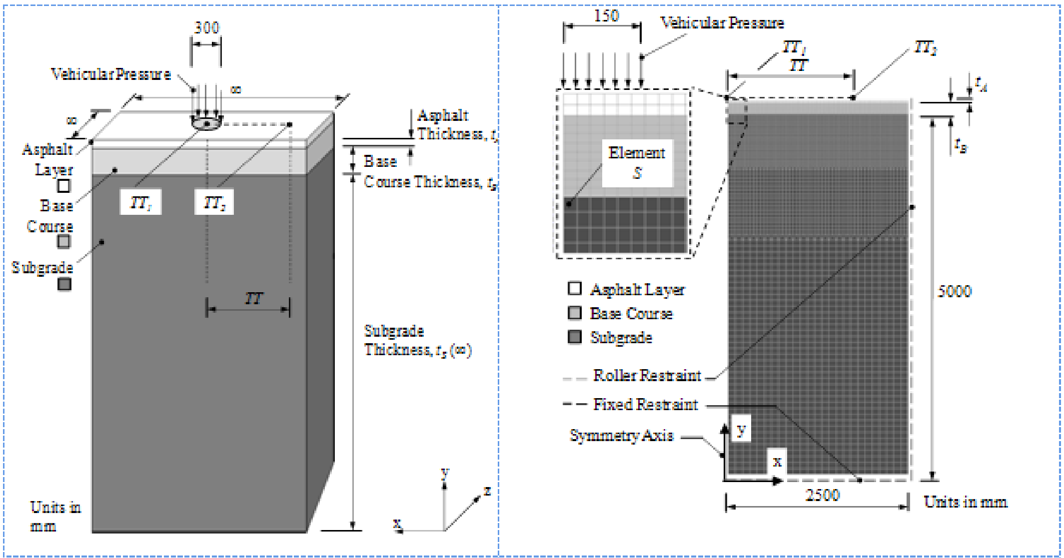

a) Model one, M_1 (LET) **b) Model two, M_2 (FEM)**

Figure 2: Loading and restraint conditions of models.

Table 1: Pavement layer thicknesses, *t* (mm) and Young's moduli, *E* (MPa)

Field Data		Model One, M_1 (LET)					Model Two, M_2 (FEM)				
		Asphalt		Base Course		Subgrade	Asphalt		Base Course		Subgrade
Set	E_S	t_A	E_A	t_B	E_B	E_S	t_A	E_A	t_B	E_B	E_S
1	30	50	2000	200	190	25	50	2000	200	160	19
2	65	40	2000	140	145	35	40	2000	140	170	26
3	170	35	3000	155	480	120	35	3000	155	600	90
4	32	50	3200	140	125	34	50	3200	140	300	20
5	160	40	3000	150	280	110	40	3000	150	400	82
6	65	55	3000	235	205	73	55	3000	235	320	41
7	140	35	4000	205	320	115	35	4000	205	472	70
8	90	50	3000	190	80	60	50	3000	190	190	32
9	90	35	3000	255	400	40	35	3000	255	400	26
10	35	40	3200	210	120	34	40	3200	210	165	20

RESULTS AND DISCUSSION

The distribution of vertical displacements in the asphalt layer is discussed for the field data, M_1 and M_2 under the applied vehicular loading. Shown in Figure 3 are the vertical displacements measured along the line *TT* and the displacement contours of M_2. Note that displacement contours of M_1 are not attainable because displacement results from ELSYM5 (Kopperman et al. 1986) are provided in text format only.

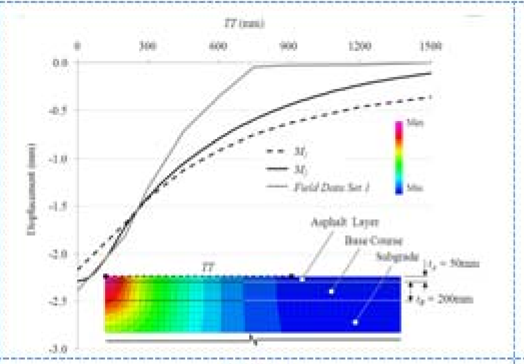

a) Set 1

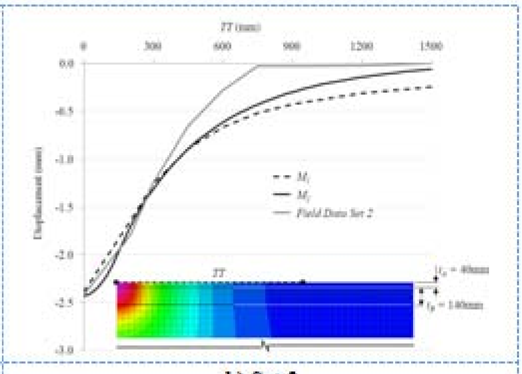

b) Set 2

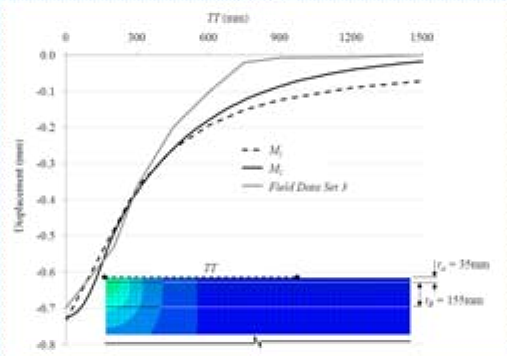

c) Set 3

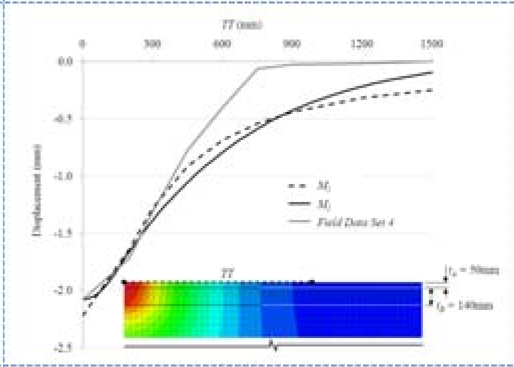

d) Set 4

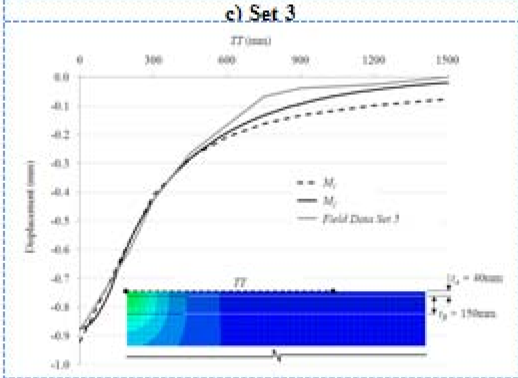

e) Set 5

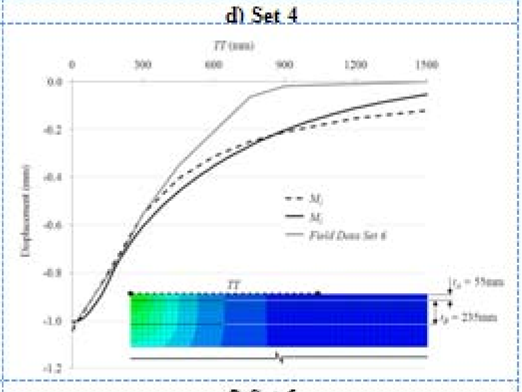

f) Set 6

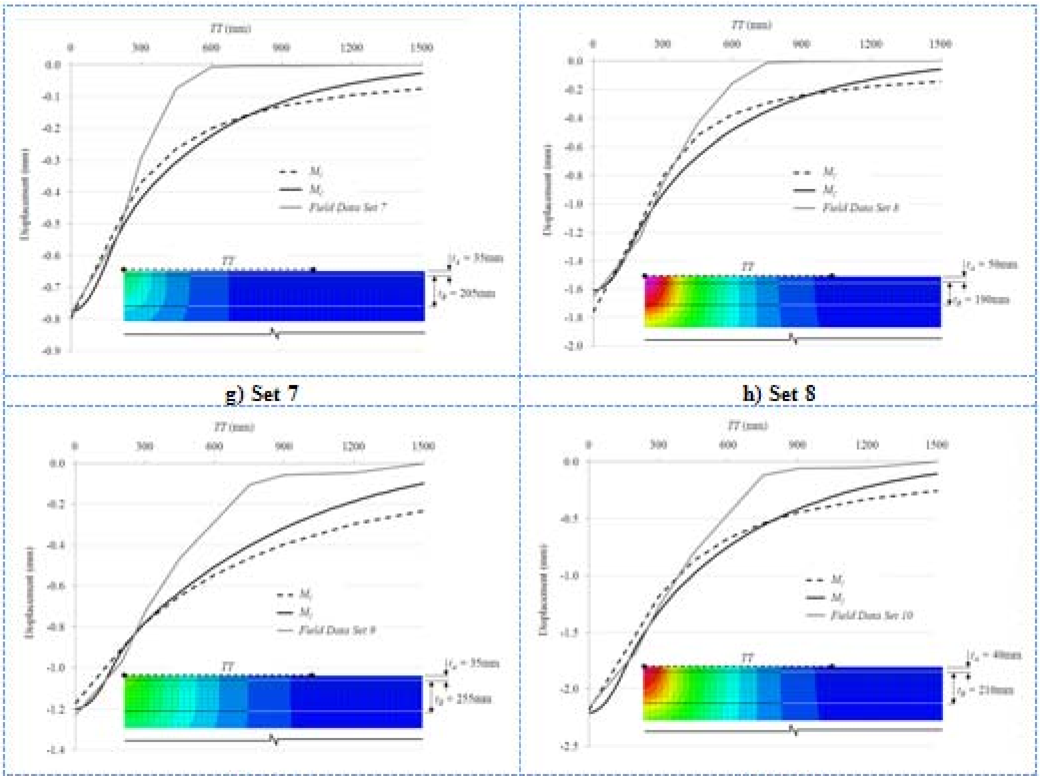

g) Set 7 h) Set 8

i) Set 9 j) Set 10

Figure 3: Comparison of vertical displacement characteristics of field data sets to M_1 and M_2.

As illustrated in Figure 3, the displacements of both models and all field data sets are relatively similar in magnitude up to 300mm from TT_1. As the distance from TT_1 increases from 300 to 750mm the displacements of both models become increasingly different compared to the field data sets. At 750mm from TT_1 a sudden change in the displacement distribution occurs for all field data sets apart from data set 7 where the change occurs at both 450 and 600mm. Pre-existing plastic deformation of pavement layers could be the cause of irregular distribution patterns. Between 750 to 1500mm from TT_1 the displacement of M_1 and M_2 gradually approach the displacement values of the field data again. When comparing the displacements of both models, M_2 shows more comparable results to the field data, along a greater portion of the line *TT*. Figure 3 also illustrates that the displacement contours of M_2, under any *E* or *t*, are localised to a region approximated by the line *TT*.

As aforementioned, the nonlinear behaviour of the pavement section, from which the field data is sourced, is a justification for differences between the displacement characteristics of the measured field data and those calculated by M_1 and M_2. Further, the

reduced Young's modulus and the increased thickness of the subgrade, when compared to the asphalt and base course layers, makes it more susceptible to plastic deformation and influential to the vertical displacement at the top of the asphalt layer. It is commonly understood (Oklahoma Department of Highways 1965, Peterson and Shepherd 1972) that the vertical compressive strain at the top of the subgrade is an indicator of the amount of plastic deformation in the form of rutting, within the pavement. AUSTROADS (2004) also states that permanent deformation is largely attributed to the subgrade and that shape loss in the asphalt and base course layers is a result of a previously deformed subgrade.
It is assumed in this study that the strain produced by M_2 will be similar to that expected from the field data based on the ability of M_2 to replicate the field displacement characteristics. Therefore, the vertical compressive strain is measured on the top of the subgrade layer at element *S* of M_2 (see Figure 2 b)), and presented in Table 2.

Table 2: Vertical compressive strain on top of subgrade

Field Data Set	1	2	3	4	5	6	7	8	9	10
Vertical Compressive Strain ($\times 10^{-6}$)	3500	4500	1400	3300	900	1400	1000	2500	1500	3300

Table 2 indicates that data set 5 has the lowest magnitude of strain when compared to the other pavement data sets. It is therefore predicted that data set 5 suffers the least from plastic deformation and it can also withstand higher repeated traffic loadings. The vertical compressive strain is expected to remain low along the entire top of the subgrade because the displacements shown in Figure 3 e) are closely matched by M_2 along the full length of *TT*. The strain of data set 7 closely matches that of set 5 however the pavement section of set 7 is expected to exhibit an increased non-linear behaviour midway along *TT*. This increased non-linear behaviour is expected to occur for the other data sets (i.e. 1,2,3,4,6,8,9 and 10) as well and it is a result of the field measured displacements not being matched by M_2.

CONCLUSIONS

A pavement system consisting of an asphalt layer, base course and subgrade is modelled as a 3D model (M_1) and 2D axisymmetric model (M_2) using ELSYM5 (Kopperman et al. 1986) and Strand7 (2004) software, respectively. Similar displacement characteristics are found when comparing pavement deflection measurements from field data with those from both M_1 and M_2. However, differences in displacement magnitudes are believed to be a result of field data sets being sourced from aged and deteriorated pavement sections. The degree of plastic deformation is determined by finding the vertical compressive strains in the subgrade. It is found that data set 5 suffers the least from plastic deformations and for that reason M_1 and M_2 can more accurately replicate the displacement characteristics. Overall the displacement characteristics of M_2 follow all field data sets closer than M_1 which shows that the finite element model is more comparable to field data than the Linear Elastic Theory.

ACKNOWLEDGMENTS

A special thank you goes to the South East Queensland Climate Adaptation Research Initiative (SEQ-CARI) for financial support and Dr Xiaoming Wang from CSIRO for his intellectual contribution.

REFERENCES

Austroads (2004) Pavement Design – A Guide to the Structural Design of Road Pavements, Sydney, Australia.

Burmister DM (1943). The theory of stresses and displacements in layered systems and applications to the design of airport runways. Highway Research Board, 23, pp. 126-144.

Dondi G (1994). Three-dimensional finite element analysis of a reinforced paved road. Fifth International Conference on Geotextiles, Geomembranes, and Related Topics. 1, pp. 95-100.

Heath AC, Roesler JR, and Harvey JT (2003). Modelling Longitudinal, Corner and Transverse Cracking in Jointed Concrete Pavements. International Journal of Pavement Engineering. 4(1), pp. 51-58.

Kopperman S, Tiller G, and Tseng M (1986). ELSYM5, Interactive microcomputer version. User's Manual, Report No. FHWA-TS-87-206, Federal Highway Administration.

Lytton RL (1989). Backcalculation of Pavement Layer Properties, Nondestructive Testing of Pavements and Backcalculation of Moduli, ASTM STP 1026, American Society for Testing and Materials, Philadelphia, AJ Bush III and GY Baladi Edition.

Strand7 Pty Ltd (2004). Strand7 Theoretical Manual, Sydney, Australia.

Uddin W, Zhang D, and Fernandes F (1994). Finite element simulation of pavement discontinuities and dynamic load response. Transportation Research Record. 1448, pp. 100–106.